# University of Groningen

## The antiproliferative drug doxorubicin inhibits liver fibrosis in bile duct-ligated rats and can be selectively delivered to hepatic stellate cells in vivo

Greupink, R; Bakker, HI; Bouma, W; Reker-Smit, C; Meijer, DKF; Beljaars, L; Poelstra, K

**IMPORTANT NOTE:** You are advised to consult the publisher's version (publisher's PDF) if you wish to cite from it. Please check the document version below.

*Document Version*
Publisher's PDF, also known as Version of record

# The Antiproliferative Drug Doxorubicin Inhibits Liver Fibrosis in Bile Duct-Ligated Rats and Can Be Selectively Delivered to Hepatic Stellate Cells in Vivo

Rick Greupink, Hester I. Bakker, Wilma Bouma, Catharina Reker-Smit, Dirk K. F. Meijer, Leonie Beljaars, and Klaas Poelstra

*Groningen University Institute for Drug Exploration (GUIDE), Department of Pharmacokinetics and Drug Delivery, University of Groningen, Groningen, The Netherlands*

## ABSTRACT

Hepatic stellate cell (HSC) proliferation is a key event in liver fibrosis; therefore, pharmacological intervention with antiproliferative drugs may result in antifibrotic effects. In this article, the antiproliferative effect of three cytostatic drugs was tested in cultured rat HSC. Subsequently, the antifibrotic potential of the most potent drug was evaluated in vivo. As a strategy to overcome drug-related toxicity, we additionally studied how to deliver this drug specifically to HSC by conjugating it to the HSC-selective drug carrier mannose-6-phosphate-modified human serum albumin (M6PHSA). We investigated the effect of cisplatin, chlorambucil, and doxorubicin (DOX) on 5-bromo-2′-deoxyuridine incorporation in cultured HSC and found DOX to be the most potent drug. Treatment of bile duct-ligated (BDL) rats with daily i.v. injections of 0.35 mg/kg DOX from day 3 to 10 after BDL reduced $\alpha$-smooth muscle actin-stained area in liver sections from $8.5 \pm 0.8$ to $5.1 \pm 0.9\%$ ($P < 0.01$) and collagen-stained area from $13.1 \pm 1.3$ to $8.9 \pm 1.5\%$ ($P < 0.05$). DOX was coupled to M6PHSA, and the organ distribution of this construct (M6PHSA-DOX) was investigated. Twenty minutes after i.v. administration, $50 \pm 6\%$ of the dose was present in the livers, and colocalization of M6PHSA-DOX with HSC markers was observed. In addition, in vitro studies showed selective binding of M6PHSA-DOX to activated HSC. Moreover, M6PHSA-DOX strongly attenuated HSC proliferation in vitro, indicating that active drug is released after uptake of the conjugate. DOX inhibits liver fibrosis in BDL rats, and HSC-selective targeting of this drug is possible. This may offer perspectives for the application of antiproliferative drugs for antifibrotic purposes.

Liver fibrosis is the common response to chronic liver injury. The activated hepatic stellate cell (HSC) is generally considered as the key cell that is responsible for the excessive collagen deposition during this disease. Therefore, new antifibrotic strategies mainly focus on the discovery of drugs that inhibit stellate cell functioning (Niki et al., 1999; Eng and Friedman, 2000; Friedman, 2000; Di Sario et al., 2002; Caligiuri et al., 2003; Kurikawa et al., 2003; Rombouts et al., 2003).

Since HSC proliferation is the hallmark of liver fibrosis, the question emerges what would happen if HSC proliferation is inhibited during the fibrotic process. Cytostatic drugs are among the most potent inhibitors of cell proliferation, and effects of these drugs on wound healing are well known (Bland et al., 1984). However, to our knowledge, no attempts to test cytostatic drugs in fibrotic animals have been made. Obviously, an important concern when using such drugs is the occurrence of serious side effects in nonhepatic tissues. Even within the liver, treatment with antiproliferative drugs may result in unwanted effects. For instance, inhibition of hepatocyte proliferation may be detrimental to the renewal of functional liver parenchyma, a crucial process in the fibrotic liver (Fausto, 2004).

In recent years, HSC-selective drug carriers have become available, which allow drugs to be delivered to HSC with increased specificity (Beljaars et al., 1999, 2000, 2003). Therefore, conjugating very potent inhibitors of cell proliferation to the HSC-selective drug carrier mannose-6-phosphate-modified human serum albumin (M6PHSA) has now

**ABBREVIATIONS:** HSC, hepatic stellate cell(s); M6PHSA, mannose-6-phosphate-modified human serum albumin; DOX, doxorubicin; PBS, phosphate-buffered saline; BW, body weight; BDL, bile duct ligated/ligation; $\alpha$-sma, $\alpha$-smooth muscle actin; BrdU, 5-bromo-2′-deoxyuridine; ALT, alanine transaminase; AST, aspartate transaminase; AP, alkaline phosphatase; $\gamma$-GT, $\gamma$-glutamyltransferase; DAB, diaminobenzidine; PAGE, polyacrylamide gel electrophoresis; TNP-470, O-(chloroacetyl-carbamoyl) fumagillol.

become an option. M6PHSA has been shown to accumulate in HSC in vivo via binding to mannose-6-phosphate/insulin-like growth factor-II receptors that are up-regulated on the cell surface of activated HSC (de Bleser et al., 1995, 1996; Beljaars et al., 1999). Ligands bound to the receptor are subject to receptor-mediated endocytosis and are routed to the acidic lysosomal compartment, where degradation of the construct and subsequent release of the coupled drug may take place (Braulke and Mieskes, 1992; Dahms and Hancock, 2002). If cytostatic drugs can be targeted to the HSC by employing this strategy, this could result in a reduction of systemic side effects and may improve the applicability of potent antiproliferative agents for antifibrotic purposes in the future.

The present study first evaluates the antiproliferative effect of three cytostatic drugs in culture-activated rat HSC. Subsequently, the most promising drug from these experiments, doxorubicin (DOX), was tested in a rat experimental model for liver fibrosis to provide better rationale for its use as an antifibrotic drug. Finally, we use in vitro and in vivo techniques to investigate whether DOX can be selectively delivered to the HSC in a pharmacologically active form by coupling it to M6PHSA.

## Materials and Methods

### HSC Isolation

HSC were isolated from the livers of male Wistar rats (>400 g; Harlan, Horst, The Netherlands) according to the method of Geerts et al. (1998). After isolation, HSC were cultured at 37°C in a 95% air, 5% $CO_2$ atmosphere in Dulbecco's modified Eagle's medium with Glutamax-1 (Invitrogen, Carlsbad, CA), supplemented with 10% fetal calf serum (Cambrex Bio Science Walkersville, Inc., Walkersville, MD), 100 U/ml penicillin (Sigma, Gillingham, UK), and 100 $\mu$g/ml streptomycin (Sigma). The purity of the HSC culture was assessed after 9 days of culture in the described medium, during which HSC activation spontaneously occurs. In these cultures, always more than 95% of the cells were positive for the activated HSC marker $\alpha$-smooth muscle actin ($\alpha$-sma), as assessed by immunohistochemical staining and cell counting.

### Effect of Drugs on HSC Proliferation in Vitro

After 9 days in culture, when HSC displayed an activated phenotype, cells were seeded in 24-well plates at a density of 30,000 cells per well. Cells were incubated with various concentrations of chlorambucil (Sigma), doxorubicin (Pfizer, Capelle aan den IJssel, The Netherlands), or cisplatin (Sigma) in the presence of 10% FCS, 50 ng/ml platelet-derived growth factor-BB and 10 $\mu$M 5-bromo-2′-deoxyuridine (BrdU; Sigma) for 24 h to allow detection of proliferating cells by immunohistochemistry. BrdU incorporation was subsequently quantified by cell counting as described previously (Greupink et al., 2005).

### Antifibrotic Potential of Doxorubicin in Bile Duct-Ligated Rats

**Experimental Animals.** Male Wistar rats of 220 to 240 g were used. Animals had free access to tap water and standard lab chow (Harlan). All experiments were approved by the local committee for care and use of laboratory animals and were performed according to strict governmental and international guidelines for the use of experimental animals. Liver fibrosis was induced by ligation of the common bile duct as described previously (Beljaars et al., 1999).

**Experimental Setup.** Ten animals were subjected to bile duct ligation (BDL) under isoflurane/$N_2O/O_2$ anesthesia at day 0 of the protocol. On day 3, the animals were randomly divided into two groups and were treated with either PBS ($n = 5$) or DOX ($n = 5$) at

a dose of 0.35 mg/kg/day. A total of seven i.v. injections were given, starting on day 3 of the protocol, and the animals were sacrificed 24 h after the last injection on day 10. Three additional rats were not subjected to bile duct ligation and served as control group.

**Number of Activated HSC and the Extent of Liver Fibrosis.** The number of activated HSC in the liver was assessed by staining for $\alpha$-sma (Sigma) on 4-$\mu$m cryostat sections, according to standard indirect immunohistochemical techniques. To study the extent of fibrosis, cryostat sections of livers were stained for collagen type III (Southern Biotechnology, Birmingham, UK). In addition, formalin-fixed paraffin-embedded tissue samples were stained with picro-sirius red dye to stain all collagens (Sigma). Microphotographs of both stainings were taken at an original magnification of 4 × 10. The fibrotic area per liver section was quantified by morphometric analysis of the sections using the Image J software package (National Institutes of Health, Bethesda, MD). Secondary to the antifibrotic effects, adverse effects were also assessed. General toxicity was monitored by analysis of body weight (BW), whereas intrahepatic toxicity of DOX toward liver cells was examined by analysis of serum AST, ALT, AP, and $\gamma$-GT levels. Inflammatory cell influx in the livers was assessed by diaminobenzidine (DAB) staining as described previously (Poelstra et al., 1990; Greupink et al., 2005), as well as by evaluation of hematoxylin/eosin-stained liver sections (Poelstra et al., 1990; Greupink et al., 2005). To evaluate the effect of DOX on the bile duct epithelial cell proliferation, staining with a monoclonal antibody raised against cytokeratin 7 (Santa Cruz Biotechnology, Santa Cruz, CA) was performed, according to standard indirect immunohistochemical techniques.

**Synthesis and Characterization of M6PHSA-DOX.** M6PHSA was synthesized as described by Beljaars et al. (1999). DOX was coupled to this drug carrier via cisaconitic acid, according to the method of Shen and Ryser (1981), covalently linking the drug and the carrier via an acid-sensitive spacer, which allows drug release within the acidic lysosomal compartment of cells (Shen and Ryser, 1981). M6PHSA-DOX was subsequently purified by dialysis against PBS and size-exclusion chromatography on a HiLoad 16/60 Superdex 200 column (Amersham Biosciences, Uppsala, Sweden). After further dialysis against water, the product was lyophilized and stored at −20°C until use.

**Chemical Characterization M6PHSA-DOX.** The total amount of coupled DOX was assessed by spectrophotometric analysis (Wirth et al., 1998; Griffiths et al., 2003). In brief, the conjugate was dissolved in PBS in a concentration of 1 mg/ml. The absorption at 480 nm was measured, and the total amount of DOX in the preparation was calculated from a calibration curve. The amount of free drug was subsequently assessed on an high-performance liquid chromatography system fitted with a pump (model 510; Waters, Milford, MA), a ThermoQuest 250 × 4.6-mm 5-$\mu$m Hypersil BDS C8 column (Thermo Electron Corporation, Waltham, MA), and a UV detector (model 441; Waters) at 254 nm. A solution of 6.7 g of trisodium citrate in 760 ml of water and 240 ml of acetonitrile (pH adjusted to 4 with formic acid) was used for elution at a flow of 1 ml/min. Monomeric protein content was analyzed by standard SDS-PAGE techniques, using a 10% polyacrylamide gel. The net-negative charge of M6PHSA-DOX and control proteins was assessed by anion-exchange chromatography on a Mono Q column as described previously (Beljaars et al., 1999).

### In Vivo Distribution of DOX and M6PHSA-DOX

**In Vivo Organ Distribution of $^{125}$I-Labeled M6PHSA-DOX.** One week after BDL, animals were injected i.v. with a tracer dose of $^{125}$I-labeled M6PHSA-DOX under $O_2/N_2O$/isoflurane anesthesia. Twenty minutes after injection, blood samples were taken by heart puncture (5–10 ml), and the animals were subsequently sacrificed by bleeding after severing the aorta. Organs were harvested and processed as described previously. All of the urine present in the bladder was collected to measure the amount of radioactivity that was excreted into the urine. The organ-associated radioactivity was expressed per whole organ and was corrected for blood-derived radioactivity. The latter was calculated from the radioactivity present in

each organ of BDL rats that were injected with ^{125}I-labeled HSA, which is known to remain in the blood. The percentage of the dose of M6PHSA-DOX in blood was calculated from the amount of radioactivity in the 5- to 10-ml blood sample by extrapolation to the corresponding value for the total blood volume in rats (60 ml/kg) (Beljaars et al., 1999).

**Localization of the Untargeted and Targeted Drug.** To investigate the distribution of DOX, 20 min after i.v. injection of the uncoupled form (2 mg/kg), after injection of M6PHSA-DOX (30 mg/kg, which contains an amount of 2 mg/kg DOX), or after injection of PBS, the animals were sacrificed and 4-$\mu$m cryostat sections of liver, kidney, and heart were made. These sections were examined by fluorescence microscopy, without embedding the sections in a mounting medium first, because this may corrupt the original localization of DOX. Microphotographs were taken with an Olympus C5050 zoom digital camera and were converted to blue-scale images, so the localization of DOX could be better discerned.

**Cellular Localization of M6PHSA-DOX.** One week after BDL, animals were injected i.v. with 30 mg/kg M6PHSA-DOX. After 20 min, the animals were sacrificed and tissues were excised and frozen in isopentane at −80°C. Cryostat sections (4 $\mu$m) of liver, heart, and kidney were acetone-fixed and stained for the presence of the conjugate with an antibody directed against HSA (Cappel, Zoetermeer, The Netherlands). In addition, we investigated whether there was colocalization of the injected construct with HSC markers. To this end, double stainings were performed for HSA and HSC markers. As a marker for HSC, two monoclonal antibodies were combined: a mouse monoclonal IgG directed against desmin (Sigma) and mouse monoclonal IgG anti-glial fibrillary acidic protein (Neomarkers, Fremont, CA) (Geerts, 2001).

**In Vitro Studies with M6PHSA-DOX.** To investigate whether the in vivo binding to HSC was mediated by specific binding of M6PHSA-DOX to receptors on HSC, the protein backbone of the conjugate was labeled with ^{125}I according to the Chloramine-T method. Culture-activated HSC were exposed to 100,000 cpm of ^{125}I-labeled M6PHSA-DOX at 37°C, in the absence of a competitor for receptor binding or in the presence of either 1 mg/ml HSA or 1 mg/ml M6PHSA. After 2 h, the cell-associated radioactivity was measured on a $\gamma$-counter (Riastar; Packard Instruments, Palo Alto, CA). The effect of M6PHSA-DOX was investigated as described above for the uncoupled drugs. The cells were incubated with 10 $\mu$g/ml M6PHSA-DOX, an equivalent amount of control protein, or PBS.

**Statistical Analysis.** Results were expressed as the mean ± S.E.M. One-way analysis of variance was used to compare the means, and differences were considered statistically significant at $P < 0.05$. For statistical analysis, the SPSS software package was used (SPSS Inc., Chicago, IL).

## Results

### Effect of Drugs on HSC Proliferation in Vitro

Culture-activated rat HSC were incubated with chlorambucil, cisplatin, and doxorubicin in various concentrations. We found that all antiproliferative drugs inhibited BrdU incorporation in a dose-dependent manner (Fig. 1). Of the tested compounds, doxorubicin was the most potent inhibitor of HSC proliferation. In the concentrations used, cell morphology was not affected, as assessed by phase-contrast microscopy (data not shown), which indicates that inhibition of proliferation precedes the cytotoxic effects of these drugs.

### Antifibrotic Potential of Doxorubicin in BDL Rats

Based on the results from the in vitro study, we subsequently investigated the effect of DOX on the fibrotic process in vivo (Fig. 2). We found that, in BDL animals, treatment
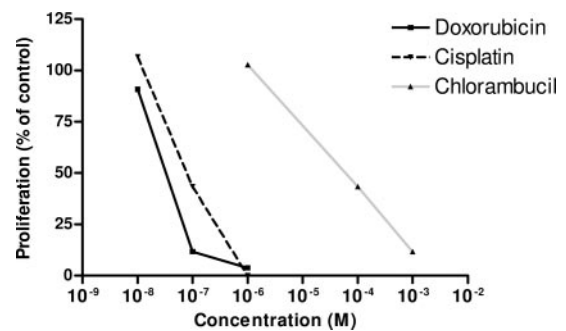


**Fig. 1.** Typical result of an experiment testing the effect of chlorambucil, cisplatin, and doxorubicin on BrdU incorporation in cultures of primary isolated culture-activated rat HSC. Data are expressed as a percentage of control.

with 0.35 mg/kg/day DOX significantly reduced the $\alpha$-sma-stained area from 8.5 ± 0.8% (PBS-treated BDL rats) to 5.1 ± 0.9% ($P < 0.01$). In normal livers, only 1.2 ± 0.2% of the total evaluated area of the liver was stained, mainly reflecting $\alpha$-sma-positive vascular smooth muscle cells in the vessel walls (Fig. 2, A–C and J). Treatment with DOX also reduced the amount of collagen, as reflected by a reduction in the collagen type III-stained area within liver sections to 8.9 ± 1.5%, compared with 13.1 ± 1.3% in PBS-treated BDL animals ($P < 0.05$). In livers of healthy control rats, only 4.9 ± 0.5% of the area was stained for collagen type III (Fig. 2, D–F and K). Sirius red staining confirmed the results of DOX on collagen deposition (Fig. 2, G–I).

Besides the antifibrotic effect of DOX, treatment with this drug also resulted in significant body weight loss. Furthermore, DOX treatment elicited increased serum $\gamma$-GT levels but not AST and ALT levels, indicating that early hepatocyte or bile duct epithelial cell injury has occurred (Table 1). Yet, the absolute number of bile duct epithelial cells, as assessed by cytokeratin 7 staining, did not differ between the PBS- and DOX-treated groups (Table 1). Moreover, evaluation of DAB stainings revealed that the number of reactive oxygen species-producing cells was also increased in the livers of DOX-treated rats (Table 1). These DAB-positive cells consisted mainly of neutrophils, judged by the presence of polymorphic nuclei in these cells after evaluation of HE-stained liver sections and based on previous studies (Poelstra et al., 1990).

### Synthesis and Characterization of M6PHSA-DOX

To increase the HSC specificity of DOX, a conjugate of this drug and M6PHSA was synthesized (Fig. 3A). Spectrophotometric analysis of the construct revealed that, per milligram of construct, 66.7 $\mu$g of doxorubicin was present. Of the total amount of doxorubicin in the preparation, only 1% was present in uncoupled form, as assessed by high-performance liquid chromatography analysis. SDS-PAGE analysis revealed that no significant amounts of polymeric protein could be detected in the conjugate (Fig. 3B). Furthermore, the net-negative charge of the conjugate was increased compared with M6PHSA and HSA, which is in agreement with molecules covalently coupled to the positively charged amine groups of HSA (Fig. 3C). The retention times measured by anion-exchange chromatography were 18.9, 26.5, and 28.0 min for HSA, M6PHSA, and M6PHSA-DOX, respectively.
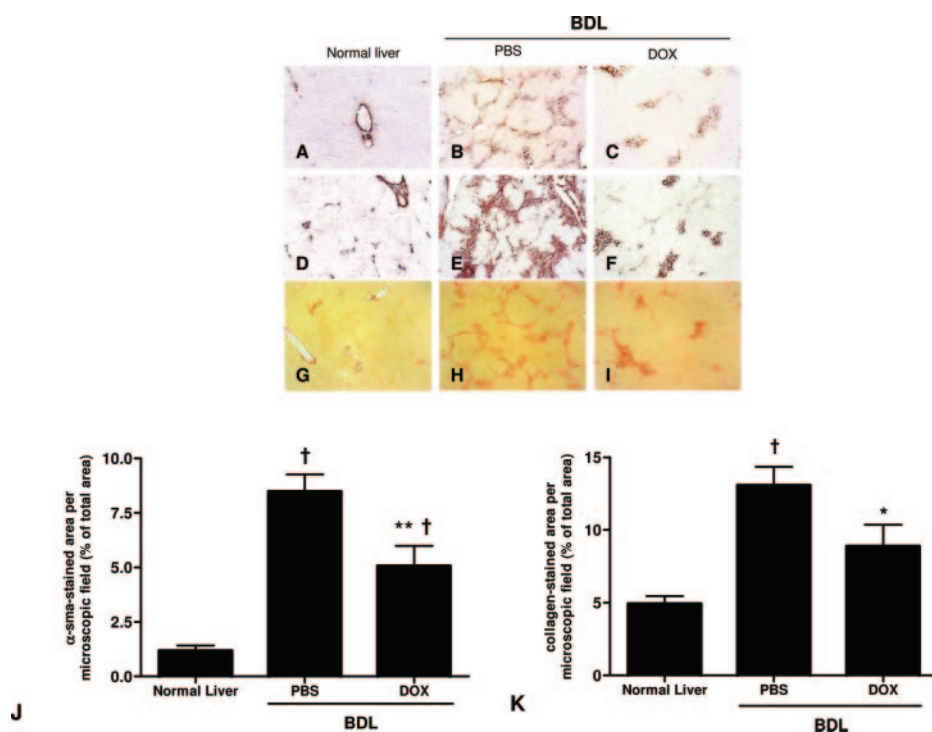
**Fig. 2.** Effect of treatment with DOX on the number of activated HSC, as assessed by $\alpha$-sma stainings (A, B, and C), and on the amount of collagen present in liver cryostat sections, as assessed by staining with an antibody directed against collagen III (D, E, and F) or with picrosirius red (G, H, and I). Representative microphotographs were taken at an original magnification of $40\times$ from the livers of healthy animals, PBS-treated BDL rats, and DOX-treated BDL rats. J, quantification of $\alpha$-sma staining by morphometric analysis. K, quantification of collagen-III-stained area by morphometric analysis. Data are expressed as mean $\pm$ S.E.M. † indicates $P < 0.01$ compared with normal rats; ∗ indicates $P < 0.05$ compared with PBS-treated BDL rats; ∗∗ indicates $P < 0.01$ compared with PBS-treated BDL rats.

TABLE 1

The effect of DOX on toxicity parameters and bile duct epithelial cell proliferation

|  | Normal | BDL | |
|---|---|---|---|
|  |  | PBS | DOX |
| $\Delta$BW (relative to BW at day 3) | N.D. | $+4.3 \pm 1.0\%$ | $-10.1 \pm 1.4\%$* |
| $\gamma$-GT (U/l) | $3 \pm 0$ | $29.83 \pm 4.98$ | $75.70 \pm 13.84$* |
| AST (U/l) | $50 \pm 5$ | $310 \pm 53$ | $391 \pm 37$ |
| ALT (U/l) | $30 \pm 2$ | $104 \pm 32$ | $89 \pm 13$ |
| AP (U/l) | $177 \pm 14$ | $436 \pm 33$ | $398 \pm 42$ |
| Inflammatory cells (number per microscopic field) | $25 \pm 1$ | $33 \pm 7$ | $97 \pm 14$* |
| Bile duct epithelial cells (% CK7-positive area per section) | $0.2 \pm 0.03$ | $3.9 \pm 0.5$ | $3.3 \pm 0.4$ |

N.D., not determined; CK7, cytokeratin 7.

* $P < 0.05$ compared with PBS-treated BDL rats.

## In Vivo Distribution of DOX and M6PHSA-DOX

**In Vivo Organ Distribution of $^{125}$I-Labeled M6PHSA-DOX.** The organ distribution of M6PHSA-DOX in rats with liver fibrosis was assessed 20 min after i.v. injection of a radiolabeled tracer dose of the conjugate. In Fig. 4, it can be seen that already $50 \pm 6\%$ of the injected dose was distributed to the liver at that time. In heart and kidney, target organs for serious side effects of doxorubicin, only $0.2 \pm 0.1$ and $1.2 \pm 0.5\%$ of the dose accumulated, respectively. In the different parts of the intestine, less than 2% of the dose was found; in addition, in the bone marrow, no significant radioactivity could be demonstrated (data not shown).

**Localization of the Untargeted and Targeted Drug.** To confirm the data of organ distribution studies that were performed with radiolabeled M6PHSA-DOX, immunohistochemical staining for HSA was performed on liver sections and sections of heart and kidney, important organs with respect to DOX toxicity. Strong staining was found in livers in a pattern consistent with accumulation in the nonparenchymal cells of the liver. In hearts and kidneys, complete absence or only minimal staining was found, respectively (Fig. 5, A–C). We also investigated the actual localization of doxorubicin itself by fluorescence microscopy at an excitation

wavelength of 450 to 490 nm and an emission filter of >515 nm, at which DOX fluoresces (Fig. 5, D–I). Administration of free DOX to fibrotic rats resulted in association of the drug with the nuclei of cardiomyocytes and with the nuclei of glomerular and tubular epithelial cells of the kidney 20 min after administration. In the livers, untargeted DOX associated with the nuclei of both hepatocytes and nonparenchymal cells. However, after coupling of DOX to M6PHSA, no DOX-specific fluorescence could be found at all in heart and kidney. Within the liver, drug-specific fluorescence was notable; animals that received M6PHSA-DOX displayed a nonparenchymal distribution pattern for the drug, with no detectable accumulation in hepatocytes.

**Cellular Localization of M6PHSA-DOX.** To examine in which liver cells the conjugate was taken up, immunohistochemical double-stainings were performed on liver sections for M6PHSA-DOX together with markers for HSC. We found that M6PHSA-DOX colocalized with HSC markers (Fig. 5M). As can be seen in the same figure, cells that were HSA-positive but negative for HSC markers were also found. Further investigation of this revealed that M6PHSA-DOX also colocalized with markers for Kupffer cells (ED2) and liver endothelial cells (RECA-1; data not shown).
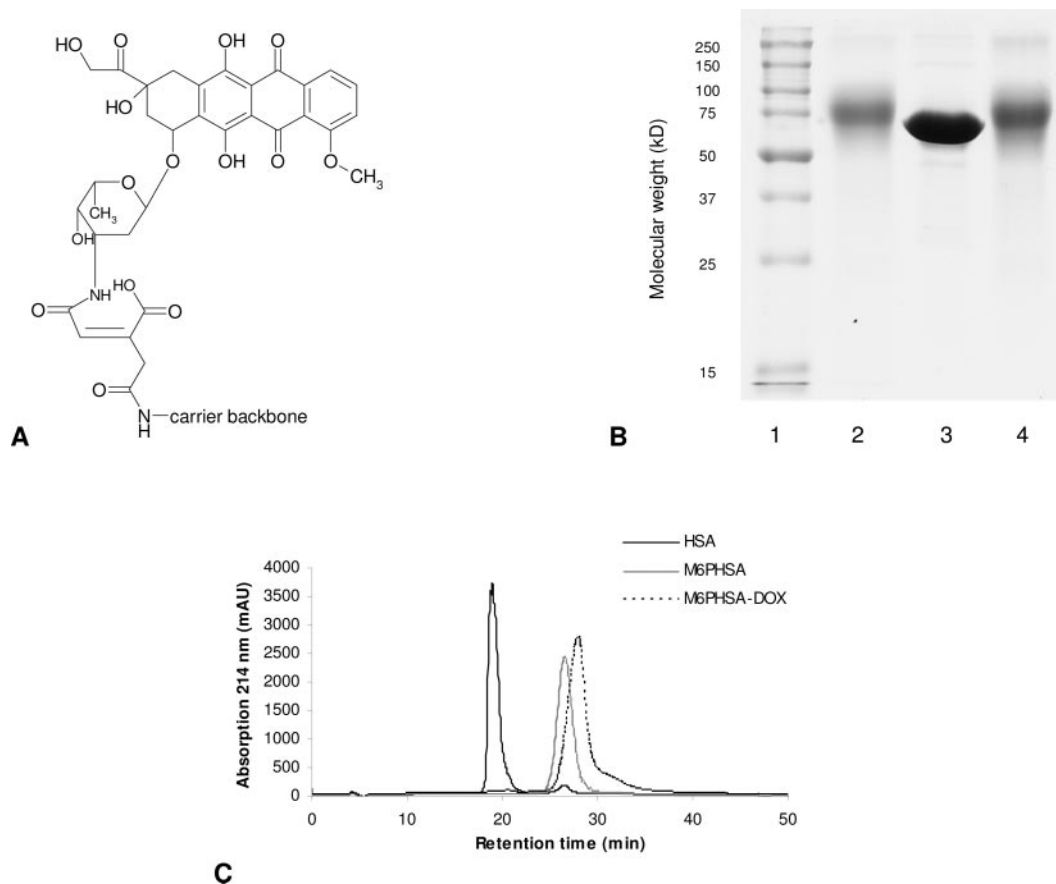
**Fig. 3.** A, schematic representation of the chemical bond between DOX and M6PHSA. B, Coomassie Brilliant Blue staining of an SDS-PAGE gel containing the drug carrier and the conjugate. Lane 1, marker; lane 2, M6PHSA-DOX; lane 3, HSA; and lane 4, M6PHSA. No significant amount of polymeric protein could be detected. C, elution profile of HSA, M6PHSA, and M6PHSA-DOX on a Mono Q anion-exchange column. Longer retention times represent an increased net negative charge.
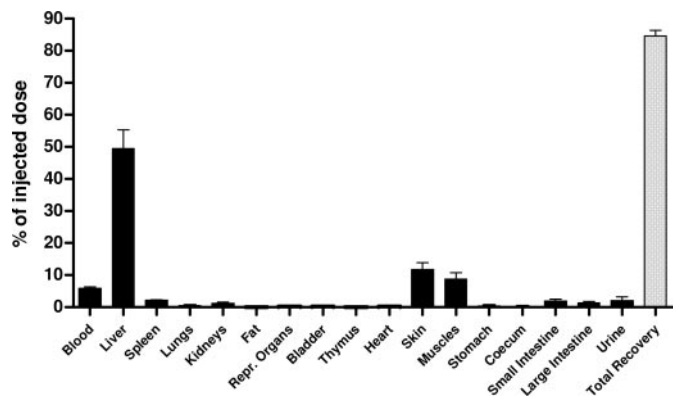


**Fig. 4.** Organ distribution of radiolabeled M6PHSA-DOX. One week after ligation of the common bile duct, animals were injected with a tracer dose of the $^{125}$I-labeled conjugate. Animals were sacrificed 20 min after injection. Data represent the average $\pm$ S.E.M. of five animals.

**In Vitro Studies with M6PHSA-DOX.** To test whether M6PHSA-DOX selectively binds to receptors on HSC, we performed binding studies on culture-activated HSC with $^{125}$I-labeled M6PHSA-DOX. In Fig. 6, it can be seen that binding to HSC was reduced by $75.2 \pm 6.3\%$ ($P < 0.05$) after coincubation with M6PHSA, which is an M6P/insulin-like growth factor-II receptor ligand. In contrast, the control protein HSA had no significant effect.

Moreover, incubation with M6PHSA-DOX reduced HSC proliferation by $82 \pm 15\%$ ($P < 0.05$), whereas the drug

carrier alone (M6PHSA) exerted no significant effect compared with vehicle-treated control cells (Fig. 7). This indicates that active drug is released after binding and uptake of the conjugate by the target cells.

## Discussion

In the present article, we show that DOX is a potent inhibitor of HSC proliferation in vitro, inhibiting cellular proliferation in the nanomolar concentration range. This is in lower concentrations than a number of other typical inhibitors of HSC proliferation in vitro, such as mycophenolic acid, statins, the selective Na$^+$/H$^+$ exchange inhibitor cariporide, and the semisynthetic analog of fumagillin TNP-470 (Wang et al., 2000; Di Sario et al., 2003; Rombouts et al., 2003; Greupink et al., 2005). The higher potency of DOX may be related to the fact that multiple intracellular mechanisms are implicated in its antiproliferative effect, in contrast to these other drugs (Gewirtz, 1999). In this article, we also show that treatment of BDL rats with doxorubicin reduces the number of activated HSC in the fibrotic rat liver and attenuates the fibrotic process. To our knowledge, this is the first study investigating the use of a cytostatic agent in an experimental model of liver fibrosis, and our data indicate that DOX, in principle, may form a new asset in the treatment of liver fibrosis for which, up until now, no pharmacotherapeutics are available. However, the observed side effects will most certainly impede its actual clinical
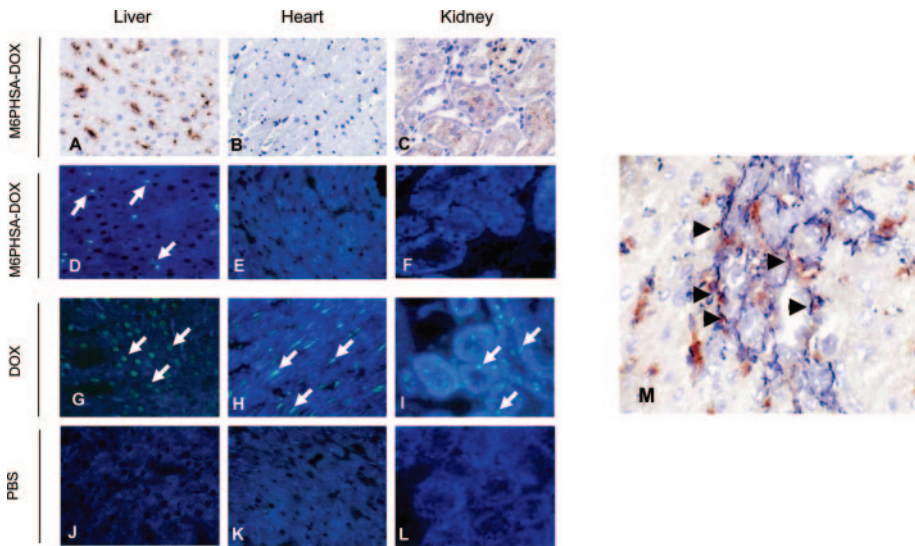
**Fig. 5.** Images of liver (A, D, and G), heart (B, E, and H), and kidney (C, F, and I) from animals receiving 30 mg/kg M6PHSA-DOX (upper two rows) or 2 mg/kg unconjugated DOX (lower row). Immunohistochemical staining for HSA (A–C) was performed to demonstrate the distribution of the drug carrier part of the conjugate (M6PHSA), and fluorescence microscopy was used to detect the drug itself (D–I). Arrows indicate the localization of DOX. Note the change in the distribution of DOX after coupling to M6PHSA compared with the uncoupled drug. In the images J, K, and L, the autofluorescence in livers, hearts, and kidneys of BDL rats is shown (original magnification 200×). M, colocalization of M6PHSA-DOX with HSC markers in the liver. The conjugate was demonstrated by immunohistochemical staining for HSA (red staining), and HSC were identified with anti-desmin/glial fibrillary acidic protein antibodies (blue staining). Arrows indicate double-positive cells. Original magnification 400×.
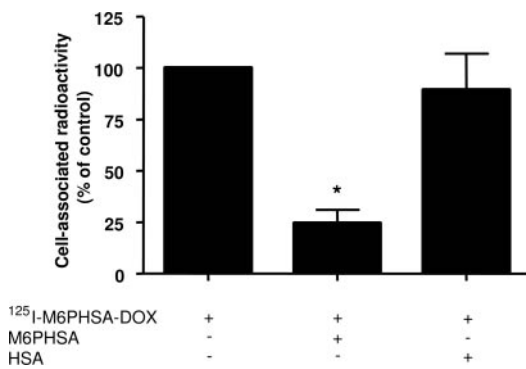


**Fig. 6.** The influence of competitors on the binding and uptake of $^{125}$I-labeled M6PHSA-DOX by culture-activated rat HSC. Note that M6PHSA, a ligand for the M6P/insulin-like growth factor-II receptor, reduces binding of the conjugate by 75.2 ± 6.5%, whereas the control protein HSA exerts no significant effect. Data represent the average ± S.E.M. of three independent experiments from three different HSC isolations. * indicates $P < 0.05$ compared with control.
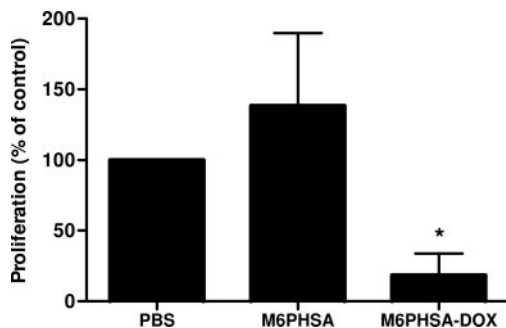


**Fig. 7.** Effect of M6PHSA and M6PHSA-DOX on HSC proliferation in vitro. * indicates $P < 0.05$ compared with control. Data represent the average ± S.E.M. of three independent experiments from three different HSC isolations.

application. In fact, toxicity is a typical problem that forms an obstacle in the application of many other promising antifibrotic drugs as well (Canbay et al., 2004; Bataller and Brenner, 2005; Hagens et al., 2005; Pinzani et al., 2005).

In this study, the toxicity of DOX was reflected by the loss in body weight, whereas the increase in serum γ-GT levels, but not AST, ALT, and AP levels, also suggested hepatocyte or bile duct epithelial cell injury. It is known

that, during the early stages of hepatocellular injury, such an isolated γ-GT increase can precede AP, ALT, or AST elevation (Moss and Henderson, 1999). Very likely, the increased number of DAB-positive cells that we observed is the result of an immune response in reaction to this damage. It is known that drug-induced hepatic inflammation can lead to liver fibrosis, but usually this takes a prolonged period of time. In the present animal model, which is characterized by a very fast proliferation of fibrogenic cells, the antiproliferative effect of DOX on these cells apparently prevails, resulting in the observed antifibrotic effect. Therefore, it would be interesting to investigate the antifibrotic potential of DOX in animal models in which fibrosis progression is slower, for example, in the CCl4 model. In this BDL model, the antifibrogenic effect of DOX was most prominent in the parenchyma and less clear in the portal areas. Whether this is due to a reduced sensitivity of portal fibroblasts to DOX or due to lower drug concentrations in this highly fibrotic area remains to be established.

Although this DOX-induced hepatic inflammation does not result in a worsening of fibrosis, it should still be considered that an even more potent antifibrotic effect can be obtained when the influx of inflammatory cells is avoided. The same may be true for the observed weight loss seen in DOX-treated rats, because it has been shown that alcohol in combination with malnutrition causes more severe liver fibrosis in rats (Bosma et al., 1994). In this way, HSC-selective delivery of DOX may not only help to avoid general drug-related toxicity but also contribute to the antifibrogenic potential of DOX via the avoidance of profibrogenic side effects.

Analysis of circulating white blood cell counts revealed no significant differences between DOX-treated BDL rats and PBS-treated BDL rats (data not shown), suggesting that no relevant myelosuppressive effect was at hand at the present dose of DOX and duration of administration. This renders it unlikely that the antifibrotic effect of DOX we describe here is mediated via the known myelosuppressive effect of the drug.

Besides the proliferation of HSC, proliferation of ductular epithelial cells occurs in the liver after ligation of the common bile duct. Our data revealed that the ductular response of

BDL rats was not significantly affected by treatment with DOX. A possible reason for this is the high expression of mdr1a drug efflux transporters in the apical membrane of the cholangiocytes (Gigliozzi et al., 2000). Because doxorubicin is a substrate for mdr1a, it is conceivable that the resistance of cholangiocytes to DOX is due to a high efflux of the drug from these cells.

To limit the effect of DOX to fibrogenic cells and to avoid the described extrahepatic and intrahepatic toxicity, we set out to investigate the targeted delivery of DOX to the HSC. From physicochemical analyses, we concluded that coupling of DOX to the HSC-selective drug carrier M6PHSA was successful. In vivo, the conjugate rapidly and selectively accumulated in the liver, whereas the untargeted drug also accumulated in organs that are prone to DOX toxicity. Within the liver, the uptake of M6PHSA-DOX was confined to the nonparenchymal cells and the observed colocalization of M6PHSA-DOX with HSC markers indicated that HSC were reached successfully. Next to the uptake in HSC, colocalization with Kupffer cell and endothelial cell markers also was observed. This very likely reflects scavenger receptor-mediated uptake of M6PHSA-DOX by these cells, because this is a highly negatively charged molecule. To attenuate uptake by these other nonparenchymal cells, the net charge of this construct should be modified. Nevertheless, we could clearly demonstrate that, although not 100% specific, injection with M6PHSA-DOX leads to a significant increase in stellate cell selectivity compared with the untargeted drug. It remains to be established whether the uptake of M6PHSA-DOX in Kupffer cells and liver endothelial cells results in toxicity or whether this contributes to the therapeutic effect of the conjugate. It is known from literature that attenuation of Kupffer cell functioning may attenuate fibrogenesis (Rivera et al., 2001).

The binding of M6PHSA-DOX to HSC was confirmed by studies performed with a ^{125}I-labeled conjugate in cultures of activated HSC. The association of radiolabeled M6PHSA-DOX with the cells could be inhibited by an excess of M6PHSA but not by HSA, indicating that receptor-mediated uptake of the construct takes place. Moreover, the strong inhibition of cell proliferation by M6PHSA-DOX that we observed also indicates that active drug can be released from the conjugate after uptake by activated HSC.

Although these results show that the targeted delivery of a cytostatic drug to the HSC is possible, it is evident that chronic treatment of fibrotic rats is necessary to test the ultimate antifibrotic potential of this targeted strategy. However, before performing those studies, it will be necessary to better understand the pharmacokinetics of M6PHSA-DOX in fibrotic animals, as well as its intracellular kinetics within HSC. Explicitly, information on the mechanisms through which this new chemical entity is processed by activated HSC and the rate at which intracellular drug release and elimination occur will largely dictate the dosage regime of M6PHSA-DOX in chronically treated rats. Based on the expected differences in cellular handling between the targeted and untargeted drug, this may be very dissimilar for the two compounds. Yet, irrespective of the eventual dosing regimen required, it is likely that, by virtue of the improved organ and cell specificity and the resulting smaller volume of distribution, the total body dose of M6PHSA-DOX can be reduced compared with untargeted DOX, whereas still similar drug concentrations can be obtained within HSC.

In summary, we have shown that treatment of BDL rats with free DOX inhibits the progression of experimental liver fibrosis and strongly inhibits HSC proliferation in vitro. Subsequently, we succeeded in delivering this potent antiproliferative drug to HSC in vitro as well as in vivo. By doing so, accumulation of DOX in extrahepatic tissues as well as hepatocytes was avoided. We conclude that DOX exerts potent antifibrotic effects in bile duct-ligated rats. In conjunction with the here-described drug delivery strategy, this may offer perspectives for the use of potent but relatively toxic antiproliferative drugs in the pharmacological treatment of liver fibrosis.

### References

Bataller R and Brenner DA (2005) Liver fibrosis. *J Clin Investig* **115:**209–218.

Beljaars L, Molema G, Schuppan D, Geerts A, de Bleser PJ, Weert B, Meijer DK, and Poelstra K (2000) Successful targeting to rat hepatic stellate cells using albumin modified with cyclic peptides that recognize the collagen type VI receptor. *J Biol Chem* **275:**12743–12751.

Beljaars L, Molema G, Weert B, Bonnema H, Olinga P, Groothuis GM, Meijer DK, and Poelstra K (1999) Albumin modified with mannose 6-phosphate: a potential carrier for selective delivery of antifibrotic drugs to rat and human hepatic stellate cells. *Hepatology* **29:**1486–1493.

Beljaars L, Weert B, Geerts A, Meijer DK, and Poelstra K (2003) The preferential homing of a platelet derived growth factor receptor-recognizing macromolecule to fibroblast-like cells in fibrotic tissue. *Biochem Pharmacol* **66:**1307–1317.

Bland KI, Palin WE, von Fraunhofer JA, Morris RR, Adcock RA, and Tobin GR (1984) Experimental and clinical observations of the effects of cytotoxic chemotherapeutic drugs on wound healing. *Ann Surg* **199:**782–790.

Bosma A, Seifert WF, van Thiel-de Ruiter GC, van Leeuwen RE, Blauw B, Roholl P, Knook DL, and Brouwer A (1994) Alcohol in combination with malnutrition causes increased liver fibrosis in rats. *J Hepatol* **21:**394–402.

Braulke T and Mieskes G (1992) Role of protein phosphatases in insulin-like growth factor II (IGF II)-stimulated mannose 6-phosphate/IGF II receptor redistribution. *J Biol Chem* **267:**17347–17353.

Caligiuri A, De Franco RM, Romanelli RG, Gentilini A, Meucci M, Failli P, Mazzetti L, Rombouts K, Geerts A, Vanasia M, et al. (2003) Antifibrogenic effects of canrenone, an antialdosteronic drug, on human hepatic stellate cells. *Gastroenterology* **124:**504–520.

Canbay A, Feldstein A, Baskin-Bey E, Bronk SF, and Gores GJ (2004) The caspase inhibitor IDN-6556 attenuates hepatic injury and fibrosis in the bile duct ligated mouse. *J Pharmacol Exp Ther* **308:**1191–1196.

Dahms NM and Hancock MK (2002) P-type lectins. *Biochim Biophys Acta* **1572:**317–340.

de Bleser PJ, Jannes P, van Buul-Offers SC, Hoogerbrugge CM, van Schravendijk CF, Niki T, Rogiers V, van den Brande JL, Wisse E, and Geerts A (1995) Insulin-like growth factor-II/mannose 6-phosphate receptor is expressed on CCl4-exposed rat fat-storing cells and facilitates activation of latent transforming growth factor-beta in cocultures with sinusoidal endothelial cells. *Hepatology* **21:**1429–1437.

de Bleser PJ, Scott CD, Niki T, Xu G, Wisse E, and Geerts A (1996) Insulin-like growth factor II/mannose 6-phosphate-receptor expression in liver and serum during acute CCl4 intoxication in the rat. *Hepatology* **23:**1530–1537.

Di Sario A, Bendia E, Svegliati BG, Ridolfi F, Casini A, Ceni E, Saccomanno S, Marzioni M, Trozzi L, Sterpetti P, et al. (2002) Effect of pirfenidone on rat hepatic stellate cell proliferation and collagen production. *J Hepatol* **37:**584–591.

Di Sario A, Bendia E, Taffetani S, Marzioni M, Candelaresi C, Pigini P, Schindler U, Kleemann HW, Trozzi L, Macarri G, et al. (2003) Selective Na$^+$/H$^+$ exchange inhibition by cariporide reduces liver fibrosis in the rat. *Hepatology* **37:**256–266.

Eng FJ and Friedman SL (2000) Fibrogenesis I. New insights into hepatic stellate cell activation: the simple becomes complex. *Am J Physiol* **279:**G7–G11.

Fausto N (2004) Liver regeneration and repair: hepatocytes, progenitor cells and stem cells. *Hepatology* **39:**1477–1487.

Friedman SL (2000) Molecular regulation of hepatic fibrosis, an integrated cellular response to tissue injury. *J Biol Chem* **275:**2247–2250.

Geerts A (2001) History, heterogeneity, developmental biology and functions of quiescent hepatic stellate cells. *Semin Liver Dis* **21:**311–335.

Geerts A, Niki T, Hellemans K, De Craemer D, Van Den Berg K, Lazou JM, Stange G, van De Winkel M, and De Bleser P (1998) Purification of rat hepatic stellate cells by side scatter-activated cell sorting. *Hepatology* **27:**590–598.

Gewirtz DA (1999) A critical evaluation of the mechanisms of action proposed for the antitumor effects of the anthracycline antibiotics adriamycin and daunorubicin. *Biochem Pharmacol* **57:**727–741.

Gigliozzi A, Fraioli F, Sundaram P, Lee J, Mennone A, Alvaro D, and Boyer JL (2000)

Molecular identification and functional characterization of Mdr1a in rat cholangiocytes. *Gastroenterology* **119:**1113–1122.

Greupink R, Bakker HI, Reker-Smit C, Loenen-Weemaes AM, Kok RJ, Meijer DK, Beljaars L, and Poelstra K (2005) Studies on the targeted delivery of the antifibrogenic compound mycophenolic acid to the hepatic stellate cell. *J Hepatol* **43:** 884–892.

Griffiths GL, Mattes MJ, Stein R, Govindan SV, Horak ID, Hansen HJ, and Goldenberg DM (2003) Cure of SCID mice bearing human B-lymphoma xenografts by an anti-CD74 antibody-anthracycline drug conjugate. *Clin Cancer Res* **9:**6567–6571.

Hagens WI, Olinga P, Meijer DKF, Grootnuis GMM, Beljaars L, and Poelstra K (2006) Gliotoxin non-selectively induces apoptosis in fibrotic and normal livers. *Liver Int* **26:**232–239.

Kurikawa N, Suga M, Kuroda S, Yamada K, and Ishikawa H (2003) An angiotensin II type 1 receptor antagonist, olmesartan medoxomil, improves experimental liver fibrosis by suppression of proliferation and collagen synthesis in activated hepatic stellate cells. *Br J Pharmacol* **139:**1085–1094.

Moss DW and Henderson AR (1999) Clinical enzymology, in *Tietz Textbook of Clinical Chemistry* (Burtis CA and Ashwood ER eds) pp 686–689, W. B. Saunders Company, Philadelphia, PA.

Niki T, Rombouts K, De Bleser P, De Smet K, Rogiers V, Schuppan D, Yoshida M, Gabbiani G, and Geerts A (1999) A histone deacetylase inhibitor, trichostatin A, suppresses myofibroblastic differentiation of rat hepatic stellate cells in primary culture. *Hepatology* **29:**858–867.

Pinzani M, Rombouts K, and Colagrande S (2005) Fibrosis in chronic liver diseases: diagnosis and management. *J Hepatol* **42 (Suppl):**S22–S36.

Poelstra K, Hardonk MJ, Koudstaal J, and Bakker WW (1990) Intraglomerular platelet aggregation and experimental glomerulonephritis. *Kidney Int* **37:**1500–1508.

Rivera CA, Bradford BU, Hunt KJ, Adachi Y, Schrum LW, Koop DR, Burchardt ER, Rippe RA, and Thurman RG (2001) Attenuation of CCl(4)-induced hepatic fibrosis by GdCl(3) treatment or dietary glycine. *Am J Physiol* **281:**G200–G207.

Rombouts K, Kisanga E, Hellemans K, Wielant A, Schuppan D, and Geerts A (2003) Effect of HMG-CoA reductase inhibitors on proliferation and protein synthesis by rat hepatic stellate cells. *J Hepatol* **38:**564–572.

Shen WC and Ryser HJ (1981) cis-Aconityl spacer between daunomycin and macromolecular carriers: a model of pH-sensitive linkage releasing drug from a lysosomotropic conjugate. *Biochem Biophys Res Commun* **102:**1048–1054.

Wang YQ, Ikeda K, Ikebe T, Hirakawa K, Sowa M, Nakatani K, Kawada N, and Kaneda K (2000) Inhibition of hepatic stellate cell proliferation and activation by the semisynthetic analogue of fumagillin TNP-470 in rats. *Hepatology* **32:**989.

Wirth M, Fuchs A, Wolf M, Ertl B, and Gabor F (1998) Lectin-mediated drug targeting: preparation, binding characteristics and antiproliferative activity of wheat germ agglutinin conjugated doxorubicin on Caco-2 cells. *Pharm Res (NY)* **15:**1031–1037.

**Address correspondence to:** Dr. R. Greupink, Antonius Deusinglaan 1, 9713 AV Groningen, The Netherlands. E-mail: a.h.greupink@rug.nl